Published in final edited form as:

Bioorg Med Chem. 2017 October 15; 25(20): 5433–5440. doi:10.1016/j.bmc.2017.07.063.

Synthesis and evaluation of analogs of 5'-(((*Z*)-4-amino-2-butenyl)methylamino)-5'-deoxyadenosine (MDL 73811, or AbeAdo) – an inhibitor of *S*-adenosylmethionine decarboxylase with antitrypanosomal activity

Anthony J. Brockway[a], **Oleg A. Volkov**[b], **Casey C. Cosner**[a], **Karen S. MacMillan**[a], **Stephen A. Wring**[c], **Thomas E. Richardson**[c], **Michael Peel**[c], **Margaret A. Phillips**[a,b,*], and **Jef K. De Brabander**[a,*]

[a]Department of Biochemistry, University of Texas Southwestern Medical Center, 5323 Harry Hines Blvd., Dallas, TX 75390-9038, USA

[b]Department of Pharmacology, University of Texas Southwestern Medical Center, 6001 Forest Park Rd., Dallas, Texas 75390-9041, USA

[c]Scynexis, Inc. (now Avista Pharma Solutions), 3501 Tricenter Blvd, Suite C, Durham, NC 27713, USA

Abstract

We describe our efforts to improve the pharmacokinetic properties of a mechanism-based suicide inhibitor of the polyamine biosynthetic enzyme *S*-adenosylmethionine decarboxylase (AdoMetDC), essential for the survival of the eukaryotic parasite *Trypanosoma brucei* responsible for Human African Trypanosomiasis (HAT). The lead compound, 5'-(((*Z*)-4-amino-2-butenyl)methylamino)-5'-deoxyadenosine (**1**, also known as MDL 73811, or AbeAdo), has curative efficacy at a low dosage in a hemolymphatic model of HAT but displayed no demonstrable effect in a mouse model of the CNS stage of HAT due to poor blood-brain barrier permeation. Therefore, we prepared and evaluated an extensive set of analogs with modifications in the aminobutenyl side chain, the 5'-amine, the ribose, and the purine fragments. Although we gained valuable structure-activity insights from this comprehensive dataset, we did not gain traction on improving the prospects for CNS penetration while retaining the potent antiparasitic activity and metabolic stability of the lead compound **1**.

Keywords

Human African Trypanosomiasis; *S*-adenosylmethionine decarboxylase; Structure-Activity relationship; antitrypanosomal; metabolism; permeability

*Corresponding authors. Margaret.Phillips@UTSouthwestern.edu and Jef.DeBrabander@UTSouthwestern.edu.

Conflict of interest

The authors declare no conflict of interest.

1. Introduction

Human African Trypanosomiasis (HAT) is caused by single-cell eukaryotic parasites *Trypanosoma brucei gambiense* and *Trypanosoma brucei rhodesiense*, with the former subspecies responsible for 97% of new registered cases.[1] After multiplying in blood and lymph of a patient, the parasite eventually transgresses the blood-brain barrier (BBB) to establish a central nervous system (CNS) infection, which causes death in most cases.[2] Four therapies are registered for HAT treatment, only two of which, melarsoprol and eflornithine (or nifurtimox-eflornithine combination therapy, NECT), are curative towards the CNS stage of the disease.[3] Both CNS-stage treatments have major shortcomings. Melarsoprol frequently causes adverse or even – in 2–5 % cases – fatal side effects, and in some areas there is evidence of resistance.[4,5] Adverse effects of NECT are less severe;[6] however, eflornithine is ineffective against the *T. b. rhodesiense* infection and is not used for its treatment.[7] Both CNS-active drugs require intravenous administration during 10 days, which is a limitation in rural areas.[5] While the number of cases has dropped over the past decade, eradication still remains a challenge. It will require safe and easy-to-administer drugs that are curative in both hemolymphatic and CNS stages of the disease.[5] Furthermore, the existence of asymptomatic human *T.b. gambiense* infections, which has only recently been discovered, further complicates control and eradication efforts.[8,9]

Polyamine biosynthesis gained recognition as a target for antitrypanosomal therapies upon the discovery by Bacchi *et al.* in 1980 that identified α-difluoromethylornithine (DFMO, eflornithine) as a curative agent against *T. brucei* infection in mice.[10] Eflornithine is a rationally designed mechanism-based suicide inhibitor of ornithine decarboxylase (ODC), which catalyzes the first committed step in polyamine biosynthesis.[3,11] Eflornithine has since been registered (both on its own and as a NECT) for treatment of late stage *T. b. gambiense* HAT confirming the polyamine pathway as a very viable target for anti-HAT drug discovery.[12,13]

S-adenosylmethionine decarboxylase (AdoMetDC) is another critical enzyme in the polyamine pathway required to generate the aminopropyl group that is then transferred onto the ODC product, putrescine, to make spermidine. Spermidine is essential in all eukaryotic cells as a substrate for the hypusine modification of the translation factor eIF5A.[14] Trypanosomatid AdoMetDC is regulated by a novel mechanism not found in mammalian cells.[11] While human AdoMetDC is a homodimer, *T. brucei* AdoMetDC requires heterodimerization with an inactive paralog termed prozyme for activity.[15,16]

Significant evidence that AdoMetDC will be a druggable target in *T. brucei* has accumulated through the finding of inhibitors with good antitrypanosomal activity.[3] The most potent of these, 5'-(((*Z*)-4-amino-2-butenyl)methylamino)-5'-deoxyadenosine (**1**, also known as MDL 73811, or AbeAdo) was designed as a mechanism-based suicide inhibitor of AdoMetDC.[17] It inhibits AdoMetDC from *E. coli*,[17] *T. brucei*,[18] rat,[19] and human,[20] acting through the enzyme-activated transamination of the covalently bound pyruvoyl prosthetic group.[20] Potential for therapeutic use of AdoMetDC inhibitors in general and **1** in particular was confirmed in a murine model of the hemolymphatic stage of HAT using *T. b. brucei* and

clinical isolates of *T. b. rhodesiense*, where it showed acutely cytostatic effect on the parasite.[18,21] Despite the activity on the mammalian enzymes, selective toxicity against *T. brucei* was obtained, and the low curative dosage in hemolymphatic model of HAT laid a solid foundation for further lead development. Unfortunately, **1** was not efficacious in a mouse model of the CNS stage of HAT[21] due to poor blood-brain barrier permeation.[19,22,23]

In attempt to improve on pharmacokinetic properties of **1**, the C8-methyl derivative Genz-644131 (**2**) was synthesized and showed about 5-fold increased activity on *T. brucei* AdoMetDC compared with **1**.[22] The improved potency on the enzyme translated to better *T. brucei* parasite growth inhibition.[22] Overall, both **1** and **2** demonstrated favorable *in vitro* and *in vivo* stability profiles.[22] However, neither of the compounds was able to achieve good CNS exposure in mice, only showing 1.7 % (**1**) and 7.3 % (**2**) brain-to-blood ratio.[22] Not surprisingly, even though both compounds resulted in sterile cure in mice infected with *T. brucei* with a 7-day 50 mg/kg/day intraperitoneal dosage,[22] neither compound led to a cure of a mouse model of the CNS stage.[21,24]

Due to the promising activity of both MDL 73811 (**1**) and Genz-644131 (**2**) (Figure 1), we embarked upon a medicinal chemistry campaign with the specific goal of improving the BBB penetration of this class of compounds. We envisioned preparing a series of compounds with structural modifications designed to increase the lipophilicity of the lead compounds, while maintaining an acceptable level of biological activity and metabolic stability.

2. Results and discussion

2.1. Synthesis and evaluation of carbamate and amide analogs

We considered that decreasing the polarity of the basic butenylamine side chain by conversion to an amide or carbamate would improve overall permeability. Thus, treatment of **2** with the appropriate 4-nitrophenyl carbonate afforded carbamates **3a–c** in good yields (Scheme 1A), whereas several terminal amide analogs **5a–c** of MDL 73811 (**1**) were prepared via alkylation of amine **4**[23] with a series of 4-amidobuten-2-yl chlorides **7a–c**, followed by acid-mediated acetal deprotection (Scheme 1B). Given that Marasco et al.[25] had shown that both enzyme inhibition and antiparasitic activity of **1** is retained after acetylation of the ribose hydroxyl groups, we also prepared the bis-acetate derivatives **6a–c** (Scheme 1B) hoping to further improve BBB penetration.

The *T. brucei* AdoMetDC enzyme inhibition, *T. b. brucei* cell growth inhibition, monolayer permeability, and both murine and human microsomal metabolic stability data are compiled in Table 1.[26] Unfortunately, none of the tested amide or carbamate derivatives retained any meaningful activity in the AdoMetDC enzyme assay, suggesting that the basic amine is essential for activity within this series. This is in agreement with the established mechanism of MDL 73811 (**1**) inhibition, which relies on the primary amine for suicide transamination of the catalytic pyruvoyl group.[20] Similarity between relative IC_{50} values assessed with and without pre-incubation in the case of the two compounds with measurable activities, **5a–b**, suggests that in the absence of the primary amine the mechanism of the enzyme inhibition is no longer time-dependent. However, we were speculating that the amides or carbamates

might act as prodrugs, but unfortunately, the lack of cellular antitrypanosomal activity indicated that no or insignificant amounts of the active parent compounds **1** or **2** were liberated within *T. b. brucei* parasites. This lack of cellular proteolytic amide or carbamate hydrolysis therefore terminates meaningful prospects for pro-drug strategies with these side-chain modifications. With the exception of benzyl carbamate **3b**, the microsomal stability of carbamates **3a,c** and amides **5a–c** was excellent, indicating that the short half-lives of the bis-acetate derivatives **6a–c** could be due to facile acetate hydrolysis. Most disappointingly however, and contrary to our original hypothesis, these changes had no positive effect on CNS delivery as measured by the MDCKII-hMDR1 monolayer permeability assay and precluded any further interest in pursuing these series.

2.2. Synthesis and evaluation of C5'-amine and ribose ketal analogs

We next explored the effects of sterics, basicity, and lipophilicity of the C5'-amine substituent in both the MDL (**8a**, R^1 = H) and Genz (**8b**, R^1 = Me) series (Scheme 2). The C5'-amine modifications (R^2) were available through Fukuyama-Mitsunobu amination of **8a,b** to afford **9a–d** in modest yields. *N*-Alkylation (→ **10a–d**) was followed by Boc deprotection to deliver **11a–d**, or simultaneous Boc and acetonide removal to afford **1** and **12b,c**. Analog **12d** was inaccessible under the later conditions due to extensive decomposition of the starting material **10d**.

The Boc- (**10a–d**) and acetonide-protected intermediates (**11a–d**) were evaluated in addition to the final deprotected analogs **12b,c** in order to compile as many SAR data points as possible (Table 2). As before, all of the analogs demonstrated severely impaired activity in the enzyme inhibition and cell growth assays, with the exception perhaps of acetonide-protected MDL 73811 (**11a**), which retained a measurable, albeit ~50-fold reduced activity (IC_{50} = 3 μM, EC_{50} = 0.42 μM) as compared to the parent MDL 73811 (**1**). Thus, we conclude that even minor increases in the size of the C5'-amine substituent (fluoroethyl **12b** or cyclopropyl **12c** versus methyl **1**) rendered this series inactive. Furthermore, this poor activity profile was matched by virtually no increase in permeability, with the exception of doubly-protected (Boc and acetonide) intermediates **10a** and **10c**. However, this significant increase in permeability was offset by extremely short microsomal half-lives. Furthermore, the several-fold difference in P_{app} values in the presence versus absence of a Pgp inhibitor suggests that these compounds are subject to undesirable Pgp-mediated efflux.

Although acetonide-protected MDL 73811 (**11a**) was less potent than the unprotected parent **1**, it still had sub-micromolar antitrypanosomal activity (0.42 μM). Therefore, we decided to briefly explore a few additional acetal analogs including the smaller methylenedioxy derivative **18**, and the more lipophilic cyclohexylidene analog **22** (Scheme 3). Synthesis of both analogs required installation of the ketal early in the synthetic route, followed by elaboration to introduce the butenyl side chain as shown in Scheme 3. Biological testing revealed that these structural changes were not well tolerated in the enzymatic (**18**: IC_{50} = 17 μM; **22**: IC_{50} >50 μM) or antiparasitic assays (**18**: EC_{50} = 21 μM; **22**: EC_{50} >25 μM). In light of these results, metabolism, permeability, and additional SAR studies were not pursued in this series.

2.3. Synthesis and evaluation of purine analogs and a trimethyl-lock prodrug

Because all attempts to identify beneficial modifications in the aminobutenyl side chain (terminal primary amine and C5'-amine) as well as ribose-diol modifications met with failure, we were compelled to redirect our efforts towards adenine SAR exploration. Our initial attention was directed at the adenine C6-amine position. Using a flexible route starting with commercially available 6-chloroadenosine (**23**), the corresponding acetonide was treated with *N*-(2-nosyl)-*N*-methylamine under Mitsunobu conditions to provide the nosyl-protected methylamine **24** in 85% yield (2 steps, Scheme 4). Subsequent S_NAr displacement of the chloride with methyl-, dimethyl-, and isopropylamine, or sodium ethoxide, followed by thiol-mediated nosyl removal furnished a series of C6-modified methylamines **25a–d** in moderate to excellent yield for this two-step process. Introduction of the *N*-Boc protected butenamine side chain (→ **26a–d**), followed by Boc-hydrolysis (→ **27**) or simultaneous Boc and acetonide deprotection (→ **28a–d**) was achieved with good overall yields using conditions previously exploited in Scheme 2. A C6-deaminated analog (i.e. **30**) was readily available via palladium-catalyzed hydrogenolysis of the C6-chloride **23**, followed by an identical series of reactions as described for the synthesis of **27**. Finally, the acetonide-protected C6-nonanamide analog **31** was available in two steps from **10a** (Scheme 2) via reaction with nonanoyl chloride and subsequent TFA-mediated Boc deprotection. All attempts at removing the ribose-acetonide for both **30** and **31** were unsuccessful, so their biological properties were benchmarked against the corresponding acetonide-protected MDL 73811 (**11a**).

As illustrated in Table 3, the C6-adenine position proved to be more tolerable for modifications, with the *N*-Me and *N*-*i*Pr derivatives **27, 28a** and **28c** only 3- to 4-fold less active against AdoMetDC compared to the unsubstituted parent MDL 73811 (**1**) or its acetonide derivative **11a** (**27** versus **11a**). The dimethylamino-substituted analog **28b** and the C6-ethoxy analog **28d** were ~20- and 16-fold less active compared to **1**. Unlike in comparators **1** and **11a**, the antitrypanosomal EC_{50} values of **27** and **28a–c** were worse than their respective enzymatic inhibition IC_{50} values, indicating a potential impairment in cellular uptake for these C6-aminoalkyl derivatives. This was not the case for nonanamide analog **31**, which *inter alia*, represents the first compound that inhibited AdoMetDC enzymatic activity and *T.b. brucei* proliferation more potently (3.5- and 2.6-fold, respectively) than the comparator compound **11a**. As noted above, we were unable to identify conditions to remove the ribose-acetonide in **31**, but if this improved potency translates to the acetonide-deprotected compound, it might be worthwhile reinvestigating acetonide deprotection conditions in conjunction with an expanded C6-amide analog set. Unfortunately, the primary objective of increasing permeability to useful levels was not achieved in any of the tested analogs, even with the addition of significant lipophilic character. Also, microsomal stability was seriously compromised for the amide analog **31**.

The final region for SAR exploration revolved around the purine ring system in an endeavor to increase the molecular lipophilicity by removal of one or more of the purine ring nitrogens. An attempted synthesis of aminobenzimidazole **40** began with reduction of 2,6-dinitroaniline (**32**) and subsequent condensation with formic acid to afford nitrobenzimidazole **34**. Displacement of the anomeric acetate of ribofuranose tetracetate

(TAR) with nitrobenzimidazole **34** yielded coupled product **35** in 95% yield. Following protecting group interconversions, the nitro-group in **36** was reduced and the primary alcohol protected as silyl ether **37**. Boc-protection and fluoride-mediated desilylation (→**38**, 57% yield) set the stage for introduction of the aminobutenyl side chain as before to provide protected analog **39** in 33% yield for this 3-step sequence. Unfortunately, and despite an exhaustive exploration of deprotection conditions, we were unable to obtain any trace of fully deprotected analog **40** and decomposition of starting material was observed in all cases.[27]

Efforts to prepare the 7-deazapurine analog **47** began with iodination of **41a** and subsequent coupling of **41b** with 1-*O*-acetyl-2,3,5-tri-*O*-benzoyl-β-*D*-ribofuranose (TBR) to afford **42** in 54% yield (Scheme 6). Treatment with NH_4OH concomitantly cleaved the benzoyl groups while installing the desired C4-amine (→**43**, 57% yield). Hydrogenative deiodination was followed with acetonide formation and TBS protection to afford **44** in 41% yield for this 3-step sequence. Subsequent bis-Boc protection of the free amine and TBS cleavage (→**45**) then enabled a 2-step installation of the aminobutenyl side chain after activation of the primary alcohol as a mesylate as before. Unfortunately, this protected 7-deaza-analog **46** proved to be as recalcitrant to deprotection as **39**, and we were unable to isolate any deprotected 7-deaza-analog **47**.[27]

Given our failed efforts thus far to improve BBB permeability while maintaining acceptable levels of *T. brucei* AdoMetDC enzyme inhibition or antitrypanosomal activity, we made an effort to explore a pro-drug approach. We settled on the trimethyl lock system first developed by Cohen and coworkers due to its successful documented use with polar primary amines.[28–30] Thus, pro-drug **49** was prepared from analog **11a** via peptide coupling with commercially available acid **48** (Scheme 7). If sufficient amounts of **49** would be able to pass through the blood-brain barrier, then local esterase activity could hydrolyze the phenolic acetate as a prelude to a Thorpe-Ingold driven lactonization to release the active, polar free amine in the brain.[28–30] While a significant drop in potency was expected (AdoMetDC IC_{50} >50 μM; 44% *T. b. brucei* inhibition at 25 μM) due to the masking of the essential terminal amine, any prospects for using **49** as a prodrug dissipated given its very short microsomal half-life (human and mouse $t_{1/2}$ = <2.5 min).

3. Conclusion

Starting from the potent AdoMetDC inhibitor MDL 73811 (**1**), we set out to design a collection of analogs to improve the ability of this antitrypanosomal compound to cross the blood-brain barrier. We explored SAR around the aminobutenyl side chain, the 5'-amine, the ribose, and adenine structural motifs. A series of amide and carbamate prodrug derivatives of the primary amine were synthesized with the prospect of increasing lipophilicity and hence the brain permeability of compounds **3a–c** and **5a–c**. Unfortunately these changes, including additional acylation of the ribose diol as in analogs **6a–c**, had no beneficial impact on predicted CNS delivery as measured by the MDCKII-hMDR1 monolayer permeability assay. Similar results were obtained with 5'-amine modified analogs (**11b–d, 12b,c**), ribose ketal analogs (**11a, 18, 22**), and adenine C6-modified analogs (**27, 28a–d, 30**). More deep-seated modifications were explored via removal of one or more nitrogen atoms from the

adenine ring, but despite extensive efforts, we were unable to identify suitable conditions to remove the Boc-protecting groups in the analog precursors **39** and **46**. Although our efforts to date have not yet led to a brain-penetrable analog, the studies described herein significantly expanded our SAR knowledge of the potent antitrypanosomal compound **1**. Most notably, we identified that acylation of the C6-adenine amine as a nonanamide provided an analog (cf. compound **31**) that actually inhibited AdoMetDC enzymatic activity and *T.b. brucei* proliferation more potently than the comparator compound **11a**. We are now focusing our efforts on preparing a larger collection of adenine C6-amide analogs and retooling our synthetic strategy in order to solve our current inability to remove the ribose acetonide in compound **31**.

4. Experimental

4.1. Biological assays

4.1.1. Materials—Unless specified, the reagents were procured from Sigma-Aldrich (St. Louis, MO, USA). *S*-adenosyl-L-methionine (AdoMet) sulfate *p*-toluenesulfonate salt was procured from Affymetrix (Santa Clara, CA, USA); HPLC-grade water, acetonitrile, and Gibco Iscove's Modified Dulbecco's Medium from Thermo Fisher Scientific (Waltham, MA, USA); ammonium formate (99% purity) from VWR International (Radnor, PA, USA); fetal bovine serum (FBS) was purchased from Atlanta Biologicals (Flowery Branch, GA, USA).

4.1.2. T. brucei AdoMetDC enzyme activity assay—The protein activity in the presence of inhibitors was assessed using mass spectrometry (MS)-based analysis of the substrate and product as previously described.[26] Briefly, the assay was initiated in a 384-well plate by combining 20 μL of the enzyme solution (50 nM purified *T. brucei* AdoMetDC/prozyme complex[15] in 100 mM Hepes, pH 7.7, 50 mM NaCl, 5 mM putrescine, 2 mM DTT, 0.1% bovine serum albumin) and 20 μL of the substrate solution (80 μM AdoMet in 100 mM Hepes, pH 7.7, 50 mM NaCl, 5 mM putrescine, 0.02% Nonidet P40 substitute) in the presence of 0.8 μ L of a compound in dimethyl sulfoxide (DMSO). A compound was added to a dry plate using Echo 555 acoustic liquid dispenser (Labcyte, Sunnyvale, CA, USA). The enzyme solution was then added when pre-incubation was indicated, and the substrate solution was added to initiate the reaction 30 min later. The order of addition of the enzyme and substrate solutions was reversed to assess inhibition without pre-incubation. The reaction was allowed to run for 20 min after combining the substrate and enzyme solutions and quenched with 40 μL of 1 M HCl.

The plates were analyzed on the RapidFire-MS system (Agilent Technologies, Santa Clara, CA, USA), specifically RapidFire 300 connected to 6430 triple quadrupole mass spectrometer as previously described.[26]

Compounds were tested at ten concentrations, typically ranging from 0.0026 to 50 μM with 3-fold dilution steps, triplicate on separate plates. Each concentration-response curve was accompanied by compound **2**-treated (fully inhibited at 10 μM) and DMSO-treated (neutral) controls. Percent conversion values for compound-treated wells were normalized to the controls (0 % and 100 % activity, respectively) to yield a percent activity. The percent activities for each concentration point in a concentration-response curve were fitted to

log(inhibitor) versus normalized response equation using nonlinear regression analysis in *Prism* (GraphPad Software, La Jolla, CA, USA) to arrive at a relative IC_{50} value.

4.1.3. T. brucei cell growth inhibition assay—*T. brucei* Lister 427 bloodstream-form (BSF) cells were cultured in HMI-19 medium[31] and the in vitro parasite growth was tested using the previously described ATP-bioluminescence cell viability assay.[26] Briefly, the assay was initiated by adding 20 μL of a 100-fold intermediate dilution of a compound in HMI-19 medium to 180 μL of cells at 3000 cells/mL in HMI-19 medium in a 96-well culture plate (CellStar, Greiner Bio-One, Monroe, NC, USA). The final DMSO concentration was 0.1%. After 48 h of culturing in the presence of a compound, 25 μL of culture were transferred to a 96-well white plate (Lumitrac 200, Greiner Bio-One) and mixed with 50 μL of CellTiter-Glo reagent (Promega, Madison, WI, USA) to assess cell viability through ATP-bioluminescence detection.[32] Compounds were tested in a concentration-response format (0.0005–3 μM or 0.0038–25 μM with 3-fold dilution steps), in triplicate. No-cell and DMSO-only controls (0% and 100% viability, respectively) were included in each plate (N=6). The data in relative luminescence units were normalized to controls in *Prism* and then fitted using nonlinear regression analysis to the log(inhibitor) versus normalized response equation to arrive at EC_{50} values.

4.1.4. In vitro metabolic stability assay—Compounds at 1 μM were incubated with male mouse or mixed-gender human liver microsomes (0.5 mg protein/mL) in the presence of NADPH at 37 °C. The LC/MS/MS samples were prepared at 0-, 5-, 10-, 20-, and 30-min time-points of incubation by taking out 50 μL, quenching with 150 μL of ice-cold acetonitrile containing labetalol (internal standard), and centrifuging. The LC separation of the supernatants was done on the Aquasil C18 DASH-HTS column (2.1 × 20 mm, 5 μm particles) (Thermo Fisher Scientific) using Agilent HPLC. Mobile phase consisted of solutions A (0.1% (*v/v*) formic acid in water) and B (5 mM ammonium formate and 0.1% (*v/v*) formic acid in methanol). A sample was eluted at 0.8 mL min with: 5 % B for 0.1 min, then linear gradient to 98 % B over 0.9 min. The eluted sample was injected into API-4000 triple quadrupole mass spectrometer (Sciex, Framingham, MA, USA) in the positive mode.

4.1.5. In vitro blood-brain barrier permeability assay—The ability of compounds to cross biological barriers, in particular BBB, was assessed in MDCKII-hMDR1 (Netherlands Cancer Institute, Amsterdam, the Netherlands) assay.[33] The cells were allowed to form confluent monolayer in a 12-well Costar Transwell plate with permeable polycarbonate membrane inserts (Corning, Lowell, MA, USA). A compound was added at 3 μM to the apical compartment, and a P-glycoprotein inhibitor GF120918 was added to both apical and basolateral compartments. Compounds were incubated with monolayers for 1 h at 160 rpm, 37 °C. The samples from both compartments were analyzed by LC/MS/MS as described above. Apparent permeability in the presence of inhibitor, P_{app}A-B (+GF918), and mass balance were calculated as described in references.[34,35] Mass balance was used as an acceptance criterion (70–120%).

4.2. Chemistry

Full experimental details, characterization of novel compounds, and copies of NMR spectra can be found in Appendix A: Supplementary data.

Supplementary Material

Refer to Web version on PubMed Central for supplementary material.

Acknowledgments

This work was supported by the National Institutes of Health (grant R01AI090599 to M.A.P. and J.K.D.B.) and the Robert A. Welch Foundation (grants I-1257 and I-1422 to M.A.P. and J.K.D.B., respectively). The authors would like to thank Dr. Melissa McCoy, Dr. Anwu Zhou, and Dr. Bruce A. Posner of the High Throughput Screening Core at UT Southwestern Medical Center for their help with running and analyzing the RapidFire-mass spectrometry enzyme assay. The authors would also like to acknowledge Shihua Zhong of the Department of Pharmacology at UT Southwestern Medical Center for performing the ATP-bioluminescence assay of parasite viability and Sara Schock of Scynexis for performing permeability assays. The Shimadzu Center for Advanced Analytical Chemistry (SCAAC) at the University of Texas at Arlington is thanked for collecting the high-resolution mass spectrometry data. J.K. De Brabander holds the Julie and Louis Beecherl, Jr., Chair in Medical Science, and M.A. Philips the Carolyn R. Bacon Professorship in Medical Science and Education and the Beatrice and Miguel Elias Distinguished Chair in Biomedical Science.

Abbreviations

AdoMet	*S*-adenosyl-L-methionine
AdoMetDC	*S*-adenosylmethionine decarboxylase
BBB	blood-brain barrier
Boc	*tert*-butoxycarbonyl
BSA	*N,O*-bis(trimethylsilyl)acetamide
CNS	central nervous system
DEAD	diethyl azodicarboxylate
DIAD	diisopropyl azodicarboxylate
DMAP	*N,N*-dimethylaminopyridine
DMF	*N,N*-dimethylformamide
DMSO	dimethyl sulfoxide
Ms	methanesulfonyl
NIS	*N*-iodosuccinimide
ODC	ornithine decarboxylase
Pgp	P-glycoprotein 1
TAR	1,2,3,5-tetra-*O*-acetyl-β-*D*-ribofuranose

TBAB	tetrabutylammonium bromide
TBAF	tetrabutylammonium fluoride
TBR	1-*O*-acetyl-2,3,5-tri-*O*-benzoyl-β-*D*-ribofuranose
TBS	*tert*-butyldimethylsilyl
Tf	trifluoromethanesulfonyl
TFA	trifluoroacetic acid
TGA	thioglycolic acid
THF	tetrahydrofuran
TMS	trimethylsilyl
Ts	*para*-toluenesulfonyl

References

1. [Accessed June 23, 2017] Lowest caseload recorded as the world prepares to defeat sleeping sickness. Apr 16. 2016 at http://www.who.int/neglected_diseases/news/HAT_lowest_caseload_recorded/en/.)
2. Kennedy PGE. Clinical features, diagnosis, and treatment of human African trypanosomiasis (sleeping sickness). Lancet Neurol. 2013; 12:186–94. [PubMed: 23260189]
3. Jacobs RT, Nare B, Phillips MA. State of the art in African trypanosome drug discovery. Curr Top Med Chem. 2011; 11:1255–74. [PubMed: 21401507]
4. Barrett MP, Boykin DW, Brun R, Tidwell RR. Human African trypanosomiasis: pharmacological re-engagement with a neglected disease. Br J Pharmacol. 2007; 152:1155–71. [PubMed: 17618313]
5. Brun R, Blum J, Chappuis F, Burri C. Human African trypanosomiasis. Lancet. 2010; 375:148–59. [PubMed: 19833383]
6. Alirol E, Schrumpf D, Amici Heradi J, et al. Nifurtimox-eflornithine combination therapy for second-stage gambiense human African trypanosomiasis: Medecins Sans Frontieres experience in the Democratic Republic of the Congo. Clin Infect Dis. 2013; 56:195–203. [PubMed: 23074318]
7. Iten M, Mett H, Evans A, Enyaru JC, Brun R, Kaminsky R. Alterations in ornithine decarboxylase characteristics account for tolerance of Trypanosoma brucei rhodesiense to D,L-alpha-difluoromethylornithine. Antimicrob Agents Chemother. 1997; 41:1922–5. [PubMed: 9303385]
8. Berthier D, Breniere SF, Bras-Goncalves R, et al. Tolerance to trypanosomatids: A threat, or a key for disease elimination? Trends Parasitol. 2016; 32:157–68. [PubMed: 26643519]
9. Jamonneau V, Ilboudo H, Kabore J, et al. Untreated human infections by Trypanosoma brucei gambiense are not 100% fatal. PLoS Negl Trop Dis. 2012; 6:e1691. [PubMed: 22720107]
10. Bacchi C, Nathan H, Hutner S, McCann P, Sjoerdsma A. Polyamine metabolism: a potential therapeutic target in trypanosomes. Science. 1980; 210:332–4. [PubMed: 6775372]
11. Willert E, Phillips MA. Regulation and function of polyamines in African trypanosomes. Trends Parasitol. 2012; 28:66–72. [PubMed: 22192816]
12. Priotto G, Kasparian S, Mutombo W, et al. Nifurtimox-eflornithine combination therapy for second-stage African Trypanosoma brucei gambiense trypanosomiasis: a multicentre, randomised, phase III, non-inferiority trial. Lancet. 2009; 374:56–64. [PubMed: 19559476]
13. Yun O, Priotto G, Tong J, Flevaud L, Chappuis F. NECT is next: implementing the new drug combination therapy for Trypanosoma brucei gambiense sleeping sickness. PLoS Negl Trop Dis. 2010; 4:e720. [PubMed: 20520803]

14. Dever TE, Gutierrez E, Shin BS. The hypusine-containing translation factor eIF5A. Crit Rev Biochem Mol Biol. 2014; 49:413–25. [PubMed: 25029904]
15. Velez N, Brautigam CA, Phillips MA. Trypanosoma brucei S-adenosylmethionine decarboxylase N terminus is essential for allosteric activation by the regulatory subunit prozyme. J Biol Chem. 2013; 288:5232–40. [PubMed: 23288847]
16. Willert EK, Fitzpatrick R, Phillips MA. Allosteric regulation of an essential trypanosome polyamine biosynthetic enzyme by a catalytically dead homolog. Proc Natl Acad Sci USA. 2007; 104:8275–80. [PubMed: 17485680]
17. Casara P, Marchal P, Wagner J, Danzin C. 5'-{[(Z)-4-Amino-2-butenyl]methylamino}-5'-deoxyadenosine: a potent enzyme-activated irreversible inhibitor of S-adenosyl-L-methionine decarboxylase from Escherichia coli. J Am Chem Soc. 1989; 111:9111–3.
18. Bitonti AJ, Byers TL, Bush TL, et al. Cure of Trypanosoma brucei brucei and Trypanosoma brucei rhodesiense infections in mice with an irreversible inhibitor of S-adenosylmethionine decarboxylase. Antimicrob Agents Chemother. 1990; 34:1485–90. [PubMed: 1977366]
19. Danzin C, Marchal P, Casara P. Irreversible inhibition of rat S-adenosylmethionine decarboxylase by 5′-{[(Z)-4-amino-2-butenyl]methylamino}-5′-deoxyadenosine. Biochem Pharmacol. 1990; 40:1499–503. [PubMed: 2222506]
20. Shantz LM, Stanley BA, Secrist JA, Pegg AE. Purification of human S-adenosylmethionine decarboxylase expressed in Escherichia coli and use of this protein to investigate the mechanism of inhibition by the irreversible inhibitors, 5'-deoxy-5'-[(3-hydrazinopropyl)methylamino]adenosine and 5'-{[(Z)-4-amino-2-butenyl]methylamino}-5'-deoxyadenosine. Biochemistry. 1992; 31:6848–55. [PubMed: 1637820]
21. Bacchi CJ, Nathan HC, Yarlett N, et al. Cure of murine Trypanosoma brucei rhodesiense infections with an Sadenosylmethionine decarboxylase inhibitor. Antimicrob Agents Chemother. 1992; 36:2736–40. [PubMed: 1482141]
22. Barker RH Jr, Liu H, Hirth B, et al. Novel S-adenosylmethionine decarboxylase inhibitors for the treatment of human African trypanosomiasis. Antimicrob Agents Chemother. 2009; 53:2052–8. [PubMed: 19289530]
23. Brockway AJ, Cosner CC, Volkov OA, Phillips MA, De Brabander JK. Improved Synthesis of MDL 73811 - a Potent AdoMetDC Inhibitor and Anti-Trypanosomal Compound. Synthesis. 2016; 48:2065–8. [PubMed: 27482123]
24. Bacchi CJ, Barker RH Jr, Rodriguez A, et al. Trypanocidal activity of 8-methyl-5'-{[(Z)-4-aminobut-2-enyl]-(methylamino)}adenosine (Genz-644131), an adenosylmethionine decarboxylase inhibitor. Antimicrob Agents Chemother. 2009; 53:3269–72. [PubMed: 19451291]
25. Marasco CJ, Kramer DL, Miller J, et al. Synthesis and Evaluation of Analogues of 5‘-([(Z)-4-Amino-2-butenyl]methylamino)-5‘-deoxyadenosine as Inhibitors of Tumor Cell Growth, Trypanosomal Growth, and HIV-1 Infectivity†. J Med Chem. 2002; 45:5112–22. [PubMed: 12408722]
26. Volkov OA, Cosner CC, Brockway AJ, et al. Identification of Trypanosoma brucei AdoMetDC Inhibitors Using a High-Throughput Mass Spectrometry-Based Assay. ACS Infect Dis. 2017
27. See Supporting Information for full details.
28. Milstien S, Cohen LA. Stereopopulation control. I. Rate enhancement in the lactonizations of o-hydroxyhydrocinnamic acids. J Am Chem Soc. 1972; 94:9158–65. [PubMed: 4642365]
29. Borchardt RT, Cohen LA. Stereopopulation control. III. Facilitation of intramolecular conjugate addition of the carboxyl group. J Am Chem Soc. 1972; 94:9175–82. [PubMed: 4642367]
30. Levine MN, Raines RT. Trimethyl lock: A trigger for molecular release in chemistry, biology, and pharmacology. Chem Sci. 2012; 3:2412–20. [PubMed: 23181187]
31. Li Q, Leija C, Rijo-Ferreira F, et al. GMP synthase is essential for viability and infectivity of Trypanosoma brucei despite a redundant purine salvage pathway. Mol Microbiol. 2015; 97:1006–20. [PubMed: 26043892]
32. Mackey ZB, Baca AM, Mallari JP, et al. Discovery of trypanocidal compounds by whole cell HTS of Trypanosoma brucei. Chem Biol Drug Des. 2006; 67:355–63. [PubMed: 16784460]
33. Polli JW, Wring SA, Humphreys JE, et al. Rational use of in vitro P-glycoprotein assays in drug discovery. J Pharmacol Exp Ther. 2001; 299:620–8. [PubMed: 11602674]

34. Thiel-Demby VE, Tippin TK, Humphreys JE, Serabjit-Singh CJ, Polli JW. In vitro absorption and secretory quotients: practical criteria derived from a study of 331 compounds to assess for the impact of P-glycoprotein-mediated efflux on drug candidates. J Pharm Sci. 2004; 93:2567–72. [PubMed: 15349966]

35. Troutman MD, Thakker DR. Novel experimental parameters to quantify the modulation of absorptive and secretory transport of compounds by P-glycoprotein in cell culture models of intestinal epithelium. Pharm Res. 2003; 20:1210–24. [PubMed: 12948019]

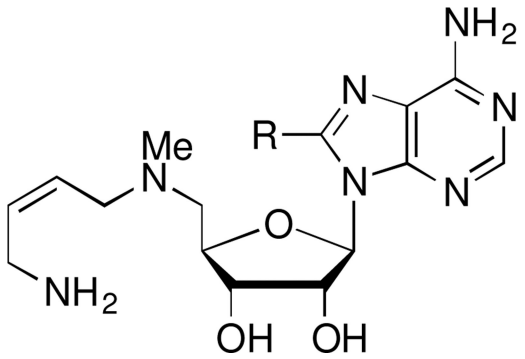

	1: R = H MDL 73811	**2**: R = Me Genz-644131
IC_{50} (AdoMetDC)	**41 nM**	**21 nM**
EC_{50} (*T. b. brucei*)	**10 nM**	**1.8 nM**
blood:brain ratio	**1.7%**	**7.3%**

Figure 1.
Structure and activity of MDL 73811 (**1**) and Genz-644131 (**2**).

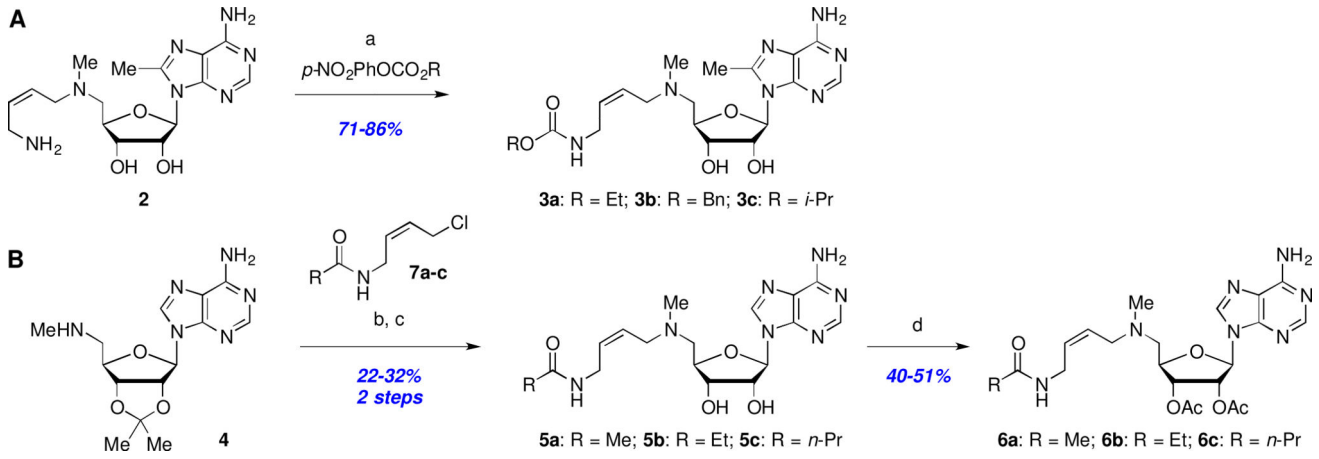

Scheme 1.

Reagents and conditions: (a) 4-NO_2-$PhOCO_2R$, Et_3N, THF, rt, 3 h; (b) **7a–c**, NaI, Et_3N, MeCN; (c) 1M H_2SO_4, MeOH; (d) Ac_2O, DMAP, MeCN.

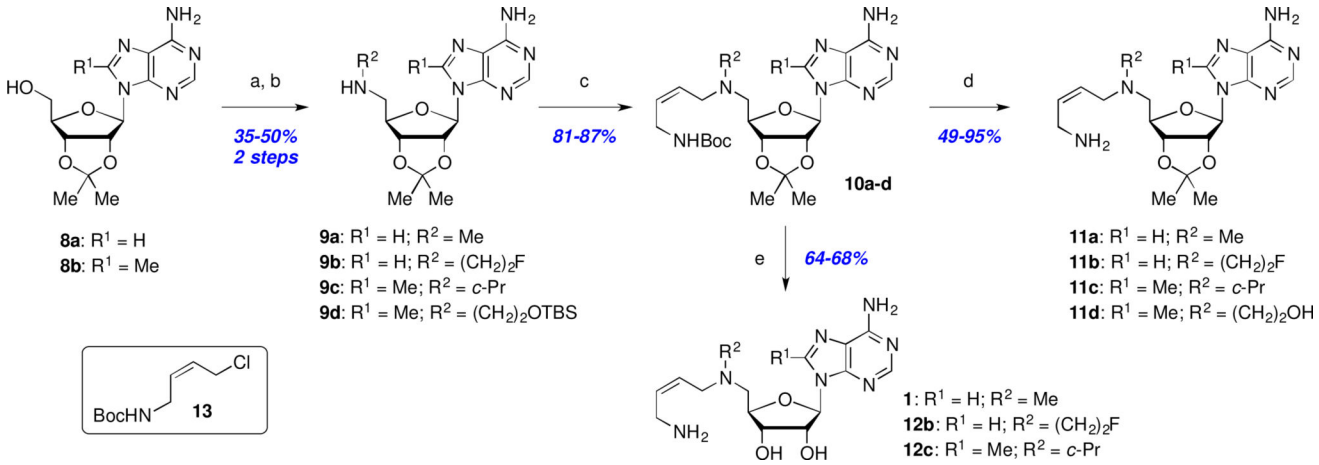

Scheme 2.

Reagents and conditions: (a) 2-NsNHR^2, DIAD, Ph_3P, THF, 0 °C to rt, 18 h; (b) TGA, LiOH, DMF, rt, 18 h; (c) *tert*-butyl (*Z*)-(4-chlorobut-2-en-1-yl)carbamate (**13**), KI, $^{i}Pr_2EtN$, MeCN; (d) TMSOTf, 2,6-lutidine *or* TFA, CH_2Cl_2, rt; (e) 4M HCl/1,4-dioxane ***or*** 1M H_2SO_4, MeOH, rt, 18 h.

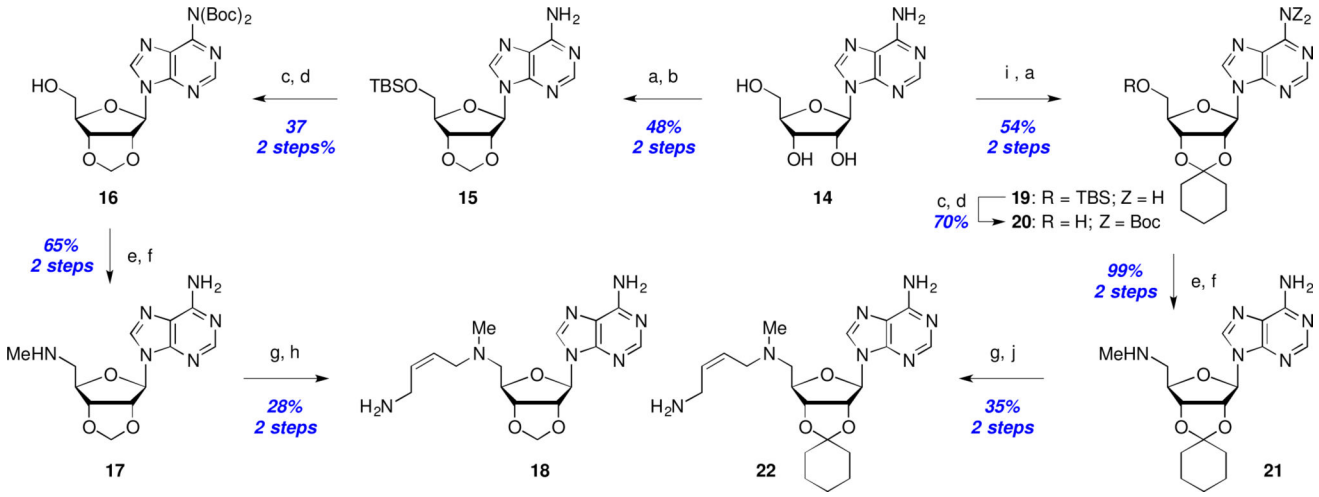

Scheme 3.

Synthesis of ribose-ketal analogs: Reagents and conditions: (a) TBSCl, imid., DMF, rt, 2–24 h; (b) CH_2Br_2, NaOH, TBAB, CH_2Cl_2/H_2O, 40 °C, 72 h; (c) Boc_2O, DMAP, DMF, 18 h; (d) TBAF, THF, 1–18 h; (e) MsCl, Et_3N, CH_2Cl_2, 1 h; (f) $MeNH_2$/EtOH, THF, 50 °C, 18 h; (g) **13**, Et_3N, NaI, MeCN, rt, 3–18 h; (h) 1M H_2SO_4, MeOH, rt, 18 h; (i) cyclohexanone, TFA, rt; (j) TFA, CH_2Cl_2, rt, 1 h.

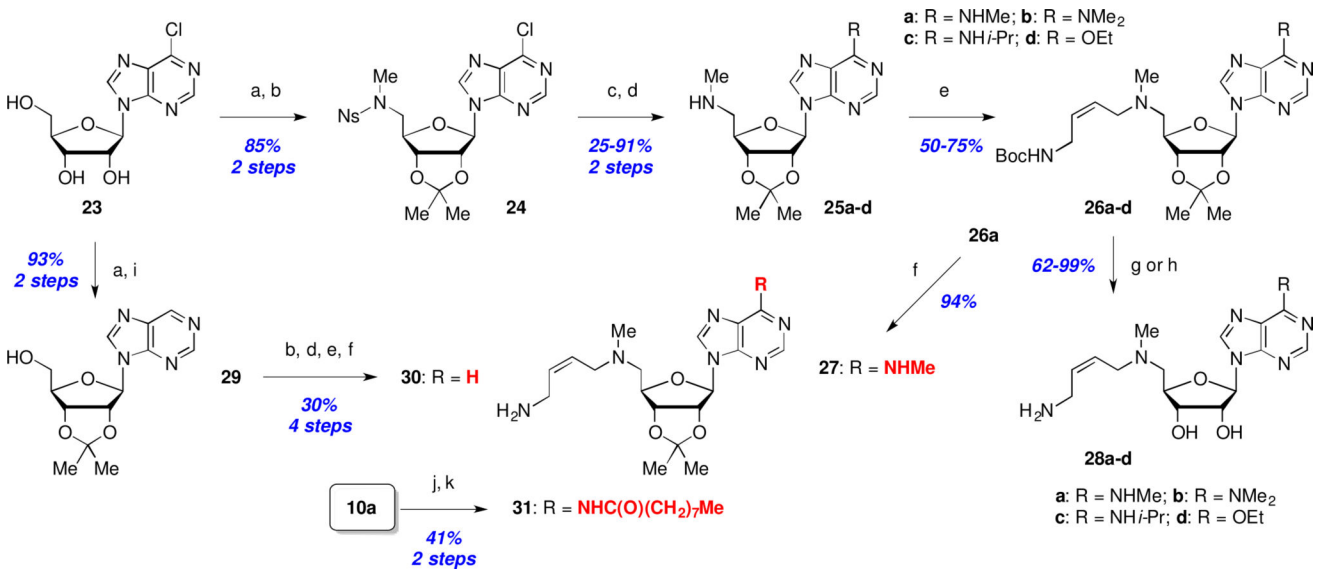

Scheme 4.

Syntheses of C6-modified analogs : Reagents and conditions: (a) $Me_2C(OMe)_2$, *p*-TsOH, acetone, rt, 2 h; (b) *N*-(2-nosyl)-*N*-methylamine, DIAD or DEAD (for **30**), Ph_3P, CH_2Cl_2, 0 °C to rt, 24 h; (c) NHRR', THF, rt or 50 °C; ***or*** EtOH, NaH, THF, 0 °C to rt, 3 h; (d) PhSH, Cs_2CO_3, MeCN, rt, 6 h; ***or*** TGA, LiOH, DMF, rt, 18 h; (e) **13**, Et_3N, NaI, MeCN, rt, 4 h; (f) TMSOTf, 2,6-lutidine, CH_2Cl_2, rt, 1 h; (g) 1M H_2SO_4, MeOH, rt, 18 h; (h) HCl, 1,4-dioxane, rt, 5 h; (i) H_2, Pd/C, K_2CO_3, THF, rt, 18 h; (j) nonanoyl chloride, Et_3N, CH_2Cl_2; (k) TFA, CH_2Cl_2.

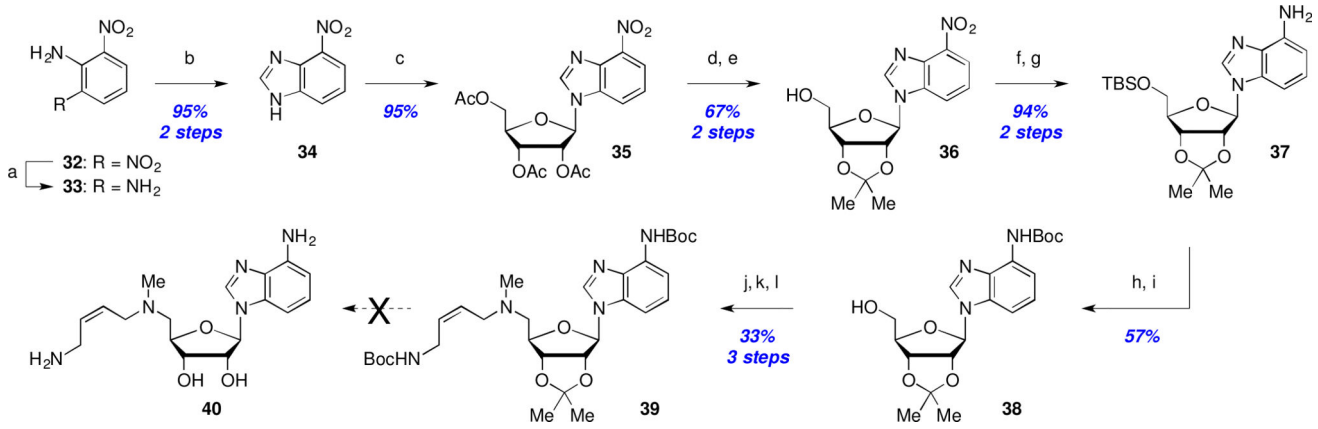

Scheme 5.

Attempted synthesis of a dideazapurine analog: Reagents and conditions: (a) Hydrazine, Ru/C, EtOH, reflux, 3 h; (b) formic acid, reflux, 18 h; (c) TAR, BSA, TMSOTf, MeCN, reflux, 3 h; (d) NH_3/MeOH; (e) $Me_2C(OMe)_2$, *p*-TsOH, 55 °C, 2 h; (f) TBSCl, imid., CH_2Cl_2; (g) Fe, $FeSO_4$, MeOH/H_2O, 50 °C, 2 h; (h) Boc_2O, DMAP, Et_3N, DMF; (i) TBAF, THF; (j) MsCl, Et_3N, CH_2Cl_2; (k) $MeNH_2$/EtOH, 50 °C, 18 h; (l) **13**, NaI, Et_3N, MeCN, rt, 6 h.

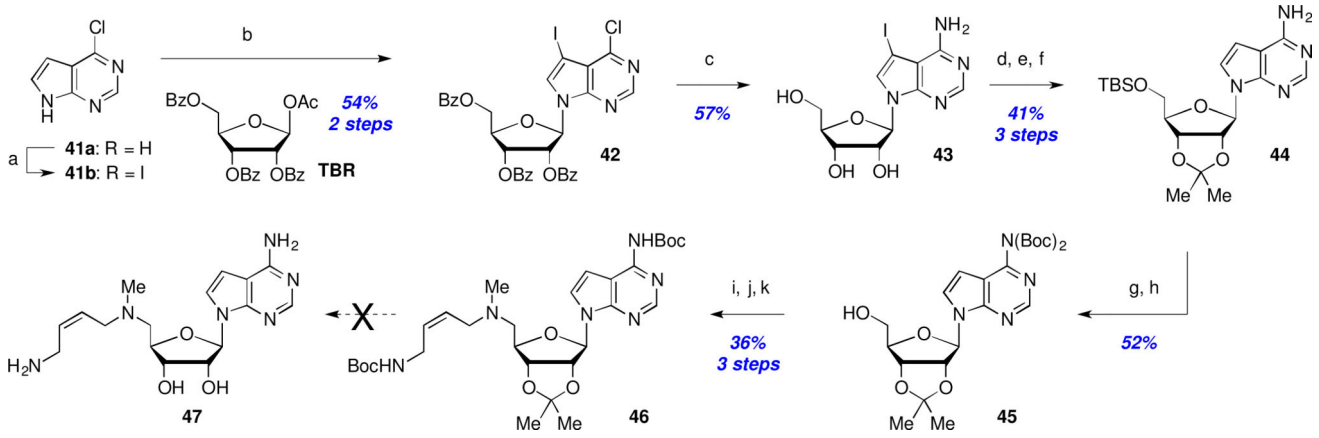

Scheme 6.

Attempted synthesis of a 7-deazapurine analog: Reagents and conditions: (a) NIS, DMF, rt, 18 h; (b) 1-*O*-acetyl-2,3,5-tri-*O*-benzoyl-β-*D*-ribofuranose (TBR), BSA, TMSOTf, MeCN, reflux, 2 h; (c) NH_4OH, 1,4-dioxane, 60 °C, 3 d; (d) H_2, Pd/C, Et_3N, DMF; (e) $Me_2C(OMe)_2$, *p*-TsOH; (f) TBSCl, imidazole, rt, 18 h; (g) Boc_2O, DMAP, Et_3N, DMF; (h) TBAF; (i) MsCl, Et_3N, CH_2Cl_2, 0.5 h; (j) $MeNH_2$/EtOH, 50 °C, 18 h; (k) **12**, NaI, Et_3N, MeCN, rt, 18 h.

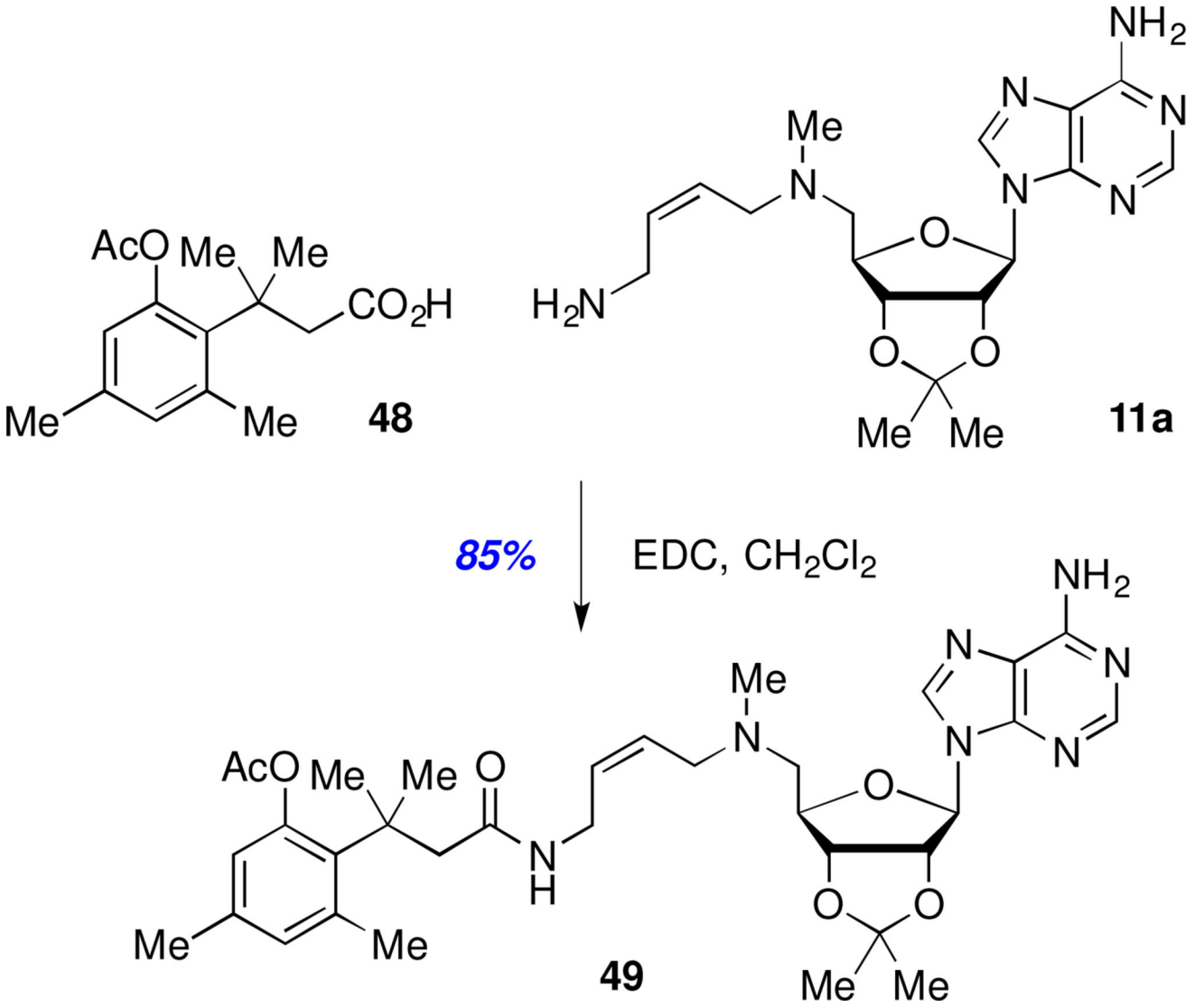

Scheme 7.
Synthesis of a trimethyl-lock prodrug.

Table 1

Enzyme and parasite growth inhibition, monolayer permeability, and microsomal stability of *N*-butenyl carbamate and amide analogs.

Cmpd	AdoMetDC IC_{50} with PI[a]	95% CI[b]	AdoMetDC IC_{50} without PI[a]	95% CI[b]	EC_{50} (*T. b. brucei*)[d]	95% CI[b]	*P*app[e] (nm/s)	S9 h/m[f] ($t_{1/2}$, min)
1	0.041 μM	(0.036–0.047)	2.4 μM	(1.9–3.1)	0.010 μM	(0.008–0.012)	7.1	>90
2	0.021 μM	(0.019–0.024)	0.23 μM	(0.18–0.30)	0.0018 μM	(0015–0.0022)	11	>90
3a	40% at 50 μM	ND[c]	40% at 50 μM	ND	40% at 25 μM	ND	12	>90
3b	39% at 50 μM	ND	17% at 50 μM	ND	2.6 μM	(1.7–3.9)	12	24/13
3c	>50 μM	ND	>50 μM	ND	35% at 25 μM	ND	10	>90
5a	18 μM	(15–21)	13 μM	(11–15)	>25 μM	ND	11	>90
5b	25 μM	(22–29)	19 μM	(16–24)	>25 μM	ND	7.2	>90
5c	>50 μM	ND	>50 μM	ND	>25 μM	ND	7.0	>90
6a	>50 μM	ND	>50 μM	ND	>25 μM	ND	7.5	>90/6.6
6b	>50 μM	ND	>50 μM	ND	>25 μM	ND	6.8	75/4.6
6c	>50 μM	ND	>50 μM	ND	>25 μM	ND	9.7	51/3.0

[a] *T. brucei* AdoMetDC/prozyme inhibition with or without 30 min pre-incubation (PI) based on triplicate data from the RapidFire-mass spectrometry-based assay as described in section *4.1.2*.

[b] Confidence Interval.

[c] Not determined.

[d] Based on triplicate data from the 48 h *T. b. brucei* cell viability assay described in section *4.1.3*.

[e] Apparent blood-brain permeability as tested in MDCKII-hMDR1 monolayer assay in the presence or absence of a P-glycoprotein 1 (Pgp) inhibitor GF120918 exactly as previously described.[26] When the two values are within <10 nm/s of each other, only permeability in the presence of the inhibitor is reported.

[f] In vitro metabolic stability presented as a half-life of a compound in human (h) or mouse (m) pooled liver microsomes (S9) measured exactly as previously described.[26] A single value is shown when the half-lives are >90 min or <2.5 min for both species.

Bioorg Med Chem. Author manuscript; available in PMC 2018 October 15.

Table 2

Enzyme and parasite growth inhibition, monolayer permeability, and microsomal stability of C5'-*N*-alkyl analogs.

Cmpd	R^1	R^2	AdoMetDC IC_{50} with PI[a]	95% CI[b]	AdoMetDC IC_{50} without PI[a]	95% CI[b]	EC_{50} (*T. b. brucei*)[d]	95% CI[b]	*P*app[e] (nm/s)	S9 h/m[f] ($t_{1/2}$, min)
10a	H	Me	>50 μM	ND[c]	>50 μM	ND	>25 μM	ND	321/51	<2.5
10c	Me	*c*-Pr	42 μM	(35–52)	>50 μM	ND	3.0 μM	(2.5–3.6)	767/312	<2.5
11a	H	Me	3.0 μM	(2.7–3.3)	22% at 50 μM	ND	0.42 μM	(0.33–0.54)	ND	>90
11b	H	$(CH_2)_2F$	>50 μM	ND	>50 μM	ND	>25 μM	ND	9.3	>90
11c	Me	*c*-Pr	>50 μM	ND	>50 μM	ND	>3 μM	ND	14	>90
11d	Me	$(CH_2)_2OH$	>50 μM	ND	>50 μM	ND	>25 μM	ND	6.8	>90
1	H	Me	0.041 μM	(0.036–0.047)	2.4 μM	(1.9–3.1)	0.010 μM	(0.008–0.012)	7.1	>90
12b	H	$(CH_2)_2F$	36% at 50 μM	ND	>50 μM	ND	>25 μM	ND	<1	>90
12c	Me	*c*-Pr	>50 μM	ND	>50 μM	ND	>3 μM	ND	10	>90

*a, b, c, d, e, f*See footnotes to Table 1.

Table 3

Enzyme and parasite growth inhibition, monolayer permeability, and microsomal stability of C6-purine analogs.

Cmpd	Purine C-6 substituent	AdoMetDC IC_{50} with PI[a]	95% CI[b]	AdoMetDC IC_{50} without PI[a]	95% CI[b]	EC_{50} (*T. b. brucei*)[d]	95% CI[b]	Papp[e] (nm/s)	S9 h/m[f] ($t_{1/2}$, min)
1	NH_2	0.041 μM	(0.036–0.047)	2.4 μM	(1.9–3.1)	0.010 μM	(0.008–0.012)	7.1	>90
11a	NH_2	3.0 μM	(2.7–3.3)	22% at 50 μM	ND	0.42 μM	(0.33–0.54)	ND	>90
27	NHMe	12 μM	(11–13)	>50 μM	ND	37% at 25 μM	ND	7.0	>90
28a	NHMe	0.17 μM	(0.15–0.20)	14 μM	(11–16)	0.37 μM	(0.23–0.58)	11.0	>90
28b	NMe_2	0.81 μM	(0.71–0.93)	37% at 50 μM	ND	10 μM	(8.4–12)	3.0	>90
28c	NH*i*Pr	0.11 μM	(0.09–0.13)	7.1 μM	(6.3–8.0)	2.5 μM	(1.9–3.1)	3.0	>90
28d	OEt	0.60 μM	(0.53–0.68)	33% at 50 μM	ND	0.36 μM	(0.29–0.44)	<1.0	>90
30	H	>50 μM	ND[c]	>50 μM	ND	>25 μM	ND	5.0	>90/59
31	$NHC(O)(CH_2)_7Me$	0.85 μM	(0.74–1.0)	48 μM	(33–69)	0.16 μM	(0.14–0.19)	24/10	9.7/6.0

*a, b, c, d, e, f*See footnotes to Table 1.

Bioorg Med Chem. Author manuscript; available in PMC 2018 October 15.